# IDENTIFICATION OF STRUCTURAL PARAMETERS FROM HELICOPTER DYNAMIC TEST DATA

Nicholas Giansante
Research Specialist

William G. Flannelly
Senior Staff Engineer

Kaman Aerospace Corporation
Bloomfield, Connecticut

## Abstract

A method is presented for obtaining the mass, stiffness, and damping parameters of a linear mathematical model, having fewer degrees of freedom than the structure it represents, directly from dynamic response measurements on the actual helicopter without a priori knowledge of the physical characteristics of the fuselage. The only input information required in the formulation is the approximate natural frequency of each mode and mobility data measured proximate to these frequencies with sinusoidal force excitation applied at only one point on the vehicle. This dynamic response information acquired from impedance testing of the actual structure over the frequency range of interest yields the second order structurally damped linear equations of motion.

The practicality and numerical soundness of the theoretical development was demonstrated through a computer simulation of an experimental program. It was shown, through approximately 400 computer experiments, that accurate system identification can be achieved with presently available measurement techniques and equipment.

## Notation

| | |
|---|---|
| C | influence coefficient |
| d | damping |
| f | force |
| $\tilde{f}$ | force phasor |
| g | structural damping coefficient |
| i | imaginary operator ($i = \sqrt{-1}$) |
| J | number of generalized coordinates |
| K | stiffness |
| m | mass |
| N | number of degrees of freedom |
| P | number of forcing frequencies |
| Q | number of modes |
| R | residual |
| S | modal mobility ratio |
| Y | displacement mobility, $\partial\tilde{y}/\partial\tilde{f}$ |
| $\Omega$ | natural frequency |
| $[\Phi]$ | matrix of modal vectors |

### Subscripts

| | |
|---|---|
| i | modal index |
| j, k | degree of freedom index, generalized coordinate index |
| ( ) | a subscripted index in parentheses means the index is held constant |

### Superscripts

| | |
|---|---|
| (q) | q-th iteration |
| * | modal parameter |
| R | real |
| I | imaginary |
| T | transpose |
| -1 | inverse |
| -T | transpose of the inverse |
| + | pseudoinverse, generalized inverse |

### Brackets

| | |
|---|---|
| [ ], ( ) | matrix |
| ⌈ ⌋ | diagonal matrix |
| { } | column or row vector |

Presented at the AHS/NASA-Ames Specialists' Meeting on Rotorcraft Dynamics, February 13-15, 1974.

capital letters under matrices indicate the number of rows and columns, respectively

a dot over a quantity indicates differentiation with respect to time

The success of a helicopter structural design is highly dependent on the ability to predict and control the dynamic response of the fuselage and mechanical components. Conventionally, this involves the formulation of intuitively based equations of motion. Ideally, this process would reduce the physical structure to an analytical mathematical model which would predict accurately the dynamic response characteristics of the actual structure. Obviously, the creation of such an intuitive abstraction of a complicated real structure requires considerable expertise and inherently includes a high degree of uncertainty. Structural dynamic testing is required to substantiate the analytical results and the analysis is modified until successful correlation is obtained between the analytical predictions and the test results.

Until a prototype vehicle is available, intuitive methods are the only choice for describing an analytical model. However, once the helicopter is built, the method of structural dynamic testing using impedance techniques can be used to define directly a dynamic model which correlates with the test data. Such a model, synthesized from test data, succeeds in unifying theory and test, minimizing the intuitive foundation of conventional analyses.

System Identification has been defined as the process of obtaining the linear equations of motion of a structure directly from test data. In System Identification the objective is the extraction of the mass, stiffness and damping parameters of a simple mathematical model directly from dynamic response measurements on the actual helicopter without a priori knowledge of the physical characteristics of the fuselage. Figure 1 presents a pictorial representation of the System Identification process.

This paper describes the theory of System Identification using impedance techniques as applied to a mathematical model having fewer degrees of freedom than the structure it represents. The method yields the mass, stiffness and damping characteristics of the structure, the influence coefficient matrix, the orthogonal modes, the exact natural frequencies, the generalized parameters associated with each mode and dynamic response fidelity over the frequency range of interest. The only information necessary to implement the method is the approximate natural frequency of each mode and mobility data measured proximate to these frequencies with the excitation applied at a single point on the vehicle. This data can be readily obtained from impedance type testing of the helicopter over the frequency spectrum of interest.

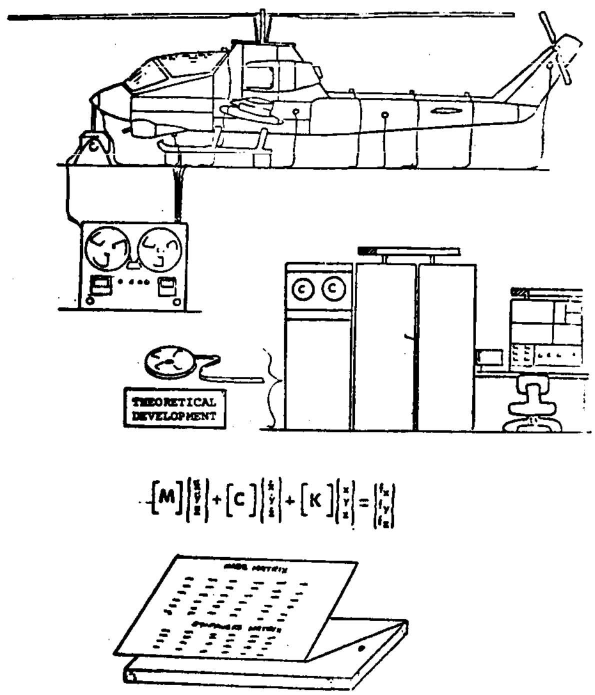


Figure 1. System Identification Process

The usefulness and numerical soundness of the theoretical development was demonstrated through a computer simulation of an experimental program, including a typical and reasonable degree of measurement error. To test the sensitivity of the method to measurement error, a series of computer experiments were conducted incorporating typical and reasonable degree of measurement error. The results indicate that accurate identification of structural parameters from dynamic test data can be achieved with presently available measurement techniques and equipment.

## Description of the Theory

### Derivation of the Single Point Iteration Process

As presented in References 1 and 2, the mobility of a structure at forcing frequency, $\omega$, is given by

$$[Y_\omega] = [\Phi] \lceil Y_{i_\omega}^* \rfloor [\Phi]^T \qquad (1)$$

With excitation at station k, the responses at station j, including k, are obtained. These provide the k-th column of the mobility at a particular forcing frequency $\omega_1$:

$$\{Y_{j(k)\omega_1}\} = \left\{ \begin{matrix} \partial y_1/\partial f_1 \\ \partial y_2/\partial f_1 \\ \vdots \\ \partial y_J/\partial f_1 \end{matrix} \right\}_{\omega_1}$$

$$= \sum_{i=1}^{N} Y_{i\omega_1}^* \phi_{ki} \{\phi\}_i = [\Phi]\{Y_{i\omega_1}^* \phi_{ki}\} \qquad (2)$$

where $1 \leq j \leq J$ and $1 \leq i \leq N$.

This represents a column of mobility response each element of which is the response at a generalized coordinate on the structure with excitation at station k and at forcing frequency $\omega_1$. Similarly, with the exciter remaining at station k, the k-th column of the mobility at another frequency, $\omega_2$, can be obtained.

$$\{Y_{j(k)\omega_2}\} = \left\{ \begin{matrix} \partial y_1/\partial f_2 \\ \partial y_2/\partial f_2 \\ \vdots \\ \partial y_J/\partial f_2 \end{matrix} \right\}_{\omega_2}$$

$$= \sum_{i=1}^{N} Y_{i\omega_2}^* \phi_{ki} \{\phi\}_i = [\Phi]\{Y_{i\omega_2}^* \phi_{ki}\} \qquad (3)$$

The columns of mobility response represented by (2) and (3) may be combined into one matrix

$$[\{Y_{j(k)\omega_1}\}\{Y_{j(k)\omega_2}\}]$$

$$= [\Phi][\{Y_{i\omega_1}^* \phi_{ki}\}\{Y_{i\omega_2}^* \phi_{ki}\}]$$

$$= \underset{J \times N}{[\Phi]} \underset{N \times N}{\lceil \phi_{ki} \rfloor} \underset{N \times 2}{[\{Y_{i\omega_1}^*\}\{Y_{i\omega_2}^*\}]} \qquad (4)$$

Generally, for p forcing frequencies where $1 \leq p \leq P$,

$$\underset{J \times P}{[Y_{j(k)p}]} = \underset{J \times N}{[\Phi]} \underset{N \times N}{\lceil \phi_{ki} \rfloor} \underset{N \times P}{[Y_{ip}^*]} \qquad (5)$$

If $J > P$, Equation (5) is set of more equations than unknowns for which there is no solution. In this situation, Equation (5) can then be written as

$$[Y_{j(k)p}] = [\Phi] \lceil \phi_{ki} \rfloor [Y_{ip}^*] + [R_{jp}] \qquad (6)$$

where $R_{jp}$ is the residual associated with the j-th station and the p-th forcing frequency.

As described in References 1 and 2, the imaginary displacement mobility is usually significantly affected by modes associated with natural frequencies in proximity to the forcing frequency. Reference 3 indicates that accurate estimates of the modal vectors may be obtained by considering only the effects of modes proximate to the forcing frequency. Therefore, the analysis will employ only Q modes, where Q is less than N. The imaginary displacement mobility may be expressed as:

$$[Y_{j(k)p}^I] = [\Phi] \lceil \phi_{ki} \rfloor [Y_{ip}^{*I}] + [R_{jp}] \qquad (7)$$

Since each column of $[Y_{ip}^{*I}]$ is associated with a particular frequency, the dominant element of each row of the matrix will be the modal mobility measured at the forcing frequency in proximity to a particular natural frequency. Normalizing the rows of the aforementioned matrix on the largest element yields

$$[S_{ip}] = \lceil 1/Y_{in}^{*I} \rfloor [Y_{ip}^{*I}] \qquad (8)$$

where $Y_{in}^{*I}$ is the maximum value of the i-th row. Equation (7) may be rewritten, incorporating Equation (8)

$$[Y^I_{j(k)p}] = [\phi][\phi_{ki}Y^{*I}_{in}][S_{ip}] + [R_{jp}] \quad (9)$$

The matrix Equation (9) has no solution, however, an approximation to a solution may be defined as that which makes the Euclidian norm of the matrix of residuals a minimum. The modal vector matrix with respect to which the Euclidian norm of the residuals is a minimum is obtained through use of the pseudoinverse, and is given by

$$[\phi] = [Y^I_{j(k)p}][S_{ip}]^+ \left[\frac{1}{\phi_{ki}Y^{*I}_{in}}\right] \quad (10)$$

where $[S_{ip}]^+$ is defined as the generalized inverse or pseudoinverse of $[S_{ip}]$ and is defined by

$$[S_{ip}]^+ = [S_{ip}]^T([S_{ip}][S_{ip}]^T)^{-1} \quad (11)$$

In Equation (10) each diagonal element of $\left[\frac{1}{\phi_{ki}Y^{*I}_{in}}\right]$ simply multiplies the corresponding column of the modal matrix. Since each modal vector is normalized on the largest element in the vector, the effect of the aforementioned multiplication is negated and Equation (10) can be reduced to

$$[\phi] = [Y^I_{j(k)p}][S_{ip}]^+ \quad (12)$$

The [S] matrix can be accurately estimated from knowledge of only the forcing frequencies and the natural frequencies. Equation (12) will be solved utilizing matrix iteration techniques. At each successive iteration a solution is found that minimizes the Euclidian norm of the residual matrix with respect to the newly found matrix of either [S] or [$\phi$]. The basic algorithm used in the matrix iteration procedure for the q-th iteration becomes

$$[\phi^{(q)}] = [Y^I][S^{(q-1)}]^+$$

and

$$[S^{(q)}] = [\phi^{(q)}]^+[Y^I] \quad (13)$$

## Determining the Modal Parameters

The real modal impedance at forcing frequency $\omega_p$ can be written as

$$Z^{*R}_{i\omega_p} = \frac{Y^{*R}_{i\omega_p}}{(Y^{*R}_{i\omega_p})^2 + (Y^{*I}_{i\omega_p})^2} \quad (14)$$

Substituting the real and imaginary displacement mobility as given in Reference 1 yields

$$Z^{*R}_{i\omega_p} = K^*_i(1 - \omega_p^2/\Omega_i^2) \quad (15)$$

From Equation (15) it is observed that the modal impedance is a linear function of the square of the forcing frequency. The forcing frequency at which the modal impedance becomes zero is, therefore, the natural frequency. From a least squares analysis of modal impedance as a function of forcing frequency squared, proximate to the natural frequency, the generalized stiffness of the i-th mode and the natural frequency of the i-th mode can be calculated.

The generalized mass associated with the i-th mode is given by

$$m^*_i = K^*_i/\Omega_i^2 \quad (16)$$

The structural damping coefficient may be determined from

$$g_i = \left(\frac{\omega_p^2}{\Omega_i^2} - 1\right)\frac{Y^{*I}_{i\omega_p}}{Y^{*R}_{i\omega_p}} \quad (17)$$

## Models

There are two basic types of dynamic mathematical models describing structures. The first type described as "Complete Models" considers as many modes as degrees of freedom. The second type labelled "Truncated Models" considers fewer modes than points of interest on the structure. Using the methods described herein, it is possible to identify either a complete model or a truncated model.

For the completed model the modal matrix [$\phi$] is square. However, in the case of the truncated model the modal matrix [$\phi$] is rectangular having J rows corresponding to the points of interest and Q columns associated with the mode shapes, where J > Q.

### Truncated Models

Consider a rectangular identified modal matrix which has J rows indicating the points of interest on the structure and Q columns representing the modes being considered where J > Q. The influence coefficient matrix for the truncated model is given by

$$[C_{TR}] = [\phi] \lceil \frac{1}{K_i^*} \rfloor [\phi]^T \qquad (18)$$

The above matrix is singular being of rank Q and order J. The mass, stiffness and damping matrices for the truncated model are

$$[m_{TR}] = [\phi]^{+T} \lceil m_i^* \rfloor [\phi]^+$$

$$[K_{TR}] = [\phi]^{+T} \lceil K_i^* \rfloor [\phi]^+$$

$$[d_{TR}] = [\phi]^{+T} \lceil g_i K_i^* \rfloor [\phi]^+ \qquad (19)$$

The classical modal eigenvalue equation has the analogous truncated form

$$[C_{TR}][m_{TR}]\{\phi_i\} = \frac{1}{\Omega_i^2}\{\phi_i\} \qquad (20)$$

### Complete Models

For the complete model the identified modal vector matrix is square, having the same number of degrees of freedom as mode shapes, thus J = Q. The influence matrix is given by

$$[C] = [\phi] \lceil 1/K_i^* \rfloor [\phi]^T = \sum_{i=1}^{N} 1/K_i^* \{\phi_i\}\{\phi_i\}^T \qquad (21)$$

The mass, stiffness and damping matrices for the complete model are similar to those of Equation (19), except that the matrices are square.

$$[m] = [\phi]^{-T} \lceil m_i^* \rfloor [\phi]^{-1}$$

$$[K] = [\phi]^{-T} \lceil 1/K_i^* \rfloor [\phi]^{-1}$$

$$[d] = [\phi]^{-T} \lceil g_i K_i^* \rfloor [\phi]^{-1} \qquad (22)$$

### Full Mobility Matrix

The full mobility matrix of either complete or truncated models is given by

$$[Y] = [\phi] \lceil Y_i^* \rfloor [\phi]^T \qquad (23)$$

### Computer Test Simulation

The usefulness and numerical soundness of the theoretical development was demonstrated through a computer simulation of an experimental program. Approximately 400 computer experiments were performed in the study. A twenty-degree-of-freedom lumped mass beam type representation of a helicopter supported on its main landing gear and tail gear was used to generate simulated mobility test data. Each of the coordinates was allowed a transverse degree of freedom. The concentrated mass and stiffness parameters of the beam are shown in Table I, with EI varying linearly between stations and with 5 percent structural damping.

### Simulated Errors

System Identification theories of any practical engineering significance must be functional with a reasonable degree of experimental error. Therefore, a typical and reasonable degree of measurement error ranging to $\pm$15% random error uniformly distributed and 15% bias error, was incorporated in the simulated test data. Both random and bias error were applied to the real and imaginary components of the displacement mobility data. The levels of error applied are consistent with those inherent in the present state-of-the-measurement art.

### Models

The number of degrees of freedom of a physical structure is infinite. Therefore, the usefulness of model identification, necessarily with a finite number of degrees of freedom, using impedance testing techniques, depends on the ability to simulate the real structure with a small mathematical model.

Several size models, containing from 5 to 15 degrees of freedom, were synthesized from the simulated test data incorporating the specified experimental error. Table II describes the various models used in the analysis. The model stations used in the models refer to the corresponding stations in the twenty point specimen.

### Identified Models

Typical generalized mass identifications are shown in Tables III, IV and V. Table III presents results for several different five point models. The model designations refer to the descriptions presented in Table II. Data are also presented for the twenty point specimen with zero experimental error. Thus, a basis of comparison is established with the theoretically exact control model of the beam representation of the helicopter. It is apparent that no outstanding differences exist among the identified generalized masses for the models considered for comparison. Table IV presents similar data for the nine-point models studied. The generalized mass distribution associated with each of the models is in excellent agreement with the twenty point model results.

Table V describes the results of the computer experiments conducted employing the twelve point models. The results are satisfactory except for the identification of the generalized masses of the tenth and eleventh modes. However, the generalized masses associated with these modes are extremely small in comparison with the remaining modal generalized masses. An examination of the tenth mode shape revealed a lack of response at all points of interest on the structure other than the first station. Therefore, the effect of the tenth mode is difficult to evaluate in the calculation of the generalized parameters. Computer experiment 309 yielded a negative generalized mass for the tenth mode. All computer experiments that failed in this respect gave drastically unrealistic values of generalized mass. Ordinarily, in a situation where the generalized mass was unrealistic, use of different stations for the model improved the identification.

TABLE I. 20-POINT SPECIMEN DESCRIPTION

| Sta No. | 1 | 2 | 3 | 4 | 5 | 6 | 7 | 8 | 9 | 10 | 11 | 12 | 13 | 14 | 15 | 16 | 17 | 18 | 19 | 20 |
|---|---|---|---|---|---|---|---|---|---|---|---|---|---|---|---|---|---|---|---|---|
| Sta (In.) | 0 | 30 | 60 | 100 | 120 | 140 | 160 | 180 | 200 | 220 | 240 | 260 | 280 | 300 | 320 | 340 | 370 | 400 | 430 | 460 |
| Mass ($Lb-Sec^2/In.$) | .029 | 1.05 | 3.67 | 3.71 | 2.18 | 2.18 | 2.385 | 2.59 | 2.08 | 1.56 | .910 | .260 | .170 | .085 | .070 | .060 | .095 | .120 | .210 | .150 |
| EI ($Lb-In.^2 \times 10^{10}$) | .35 | .35 | .35 | 1.20 | 1.95 | 3.00 | 4.37 | 5.70 | 5.80 | 5.60 | 4.425 | 3.6 | 3.07 | 2.60 | 2.05 | 1.60 | .975 | .65 | .55 | .50 |
| Springs to Ground (Lb/In.) | | | | | | 10000 | | | | | | | | | | | | 10000 | | |

TABLE II. MODEL DESCRIPTION

| Model | Stations Used 1 | 2 | 3 | 4 | 5 | 6 | 7 | 8 | 9 | 10 | 11 | 12 | 13 | 14 | 15 | 16 | 17 | 18 | 19 | 20 |
|---|---|---|---|---|---|---|---|---|---|---|---|---|---|---|---|---|---|---|---|---|
| 5A | x | | | | | x | | | | x | | | | | x | | | | | x |
| 5B | x | | | | | x | | | | | x | | | | | x | | | | x |
| 5C | x | | | | | x | | | | x | | | | | x | | | | x | |
| 5D | | x | | | | x | | | | | | x | | | x | | | | x | |
| 9A | x | x | | | | x | x | | | x | | | x | | | x | | x | | x |
| 9B | x | | x | | | x | | x | | | x | | | x | | | x | | x | x |
| 9C | | x | x | | | x | x | | | x | | | x | | | x | | x | | x |
| 12A | | x | x | x | x | x | | x | | x | | x | | x | | x | | x | | x |
| 12B | x | x | x | | x | x | | x | | x | | x | | x | | x | | x | | x |
| 12F | x | x | x | | x | x | | x | | | x | | x | | x | | x | | x | |

TABLE III. IDENTIFICATION OF GENERALIZED MASSES, 5 X 5 MODEL OF 20 X 20 SPECIMEN

| Model | 5A | 5B | 5C | 5D | 1** |
|---|---|---|---|---|---|
| Computer Experiment Number | 296 | 297 | 292 | 295 | - |
| Random Disp. Error | ±5% | ±5% | ±5% | ±5% | 0 |
| Bias Disp. Error | +5% | +5% | +5% | +5% | 0 |
| Random Error Seed | 13 | 13 | 13 | 13 | - |
| **Mode** | | | Generalized Masses ($Lb-Sec^2/In.$) | | |
| 1 | 8.544 | 8.538 | 8.543 | 8.568 | 8.534 |
| 2 | 4.506 | 4.506 | 4.619 | 4.610 | 4.449 |
| 3 | .494 | .494 | .494 | .493 | .495 |
| 4 | 1.048 | 1.047 | 1.050 | .994 | 1.087 |
| 5 | .653 | .653 | .651 | .629 | .630 |

** From 20 x 20 Specimen

TABLE IV. IDENTIFICATION OF GENERALIZED MASSES, 9 X 9 MODEL OF 20 X 20 SPECIMEN

| Model | 9A | 9B | 9C | 20 Pt |
|---|---|---|---|---|
| Computer Experiment Number | 300 | 303 | 304 | 1** |
| Random Disp. Error | ±5% | ±5% | ±5% | 0 |
| Bias Disp. Error | +5% | +5% | +5% | 0 |
| Random Error Seed | 13 | 13 | 13 | - |
| **Mode** | | Generalized Masses ($Lb-Sec^2/In.$) | | |
| 1 | 9.000 | 9.015 | 9.043 | 8.534 |
| 2 | 4.350 | 4.335 | 4.513 | 4.449 |
| 3 | .472 | .472 | .472 | .495 |
| 4 | 1.042 | 1.042 | 1.138 | 1.087 |
| 5 | .551 | .549 | .584 | .630 |
| 6 | .786 | .783 | .723 | .743 |
| 7 | 1.154 | 1.243 | 1.120 | 1.177 |
| 8 | 1.401 | 1.411 | 1.396 | 1.412 |
| 9 | .787 | .708 | .791 | .786 |

** From 20 x 20 Specimen

TABLE V. IDENTIFICATION OF GENERALIZED MASSES, 12 X 12 MODEL OF 20 X 20 SPECIMEN

| Model | 12B | 12F | 12A | 20 Pt |
|---|---|---|---|---|
| Computer Experiment Number | 312 | 311 | 309 | 1** |
| Random Disp. Error | ±5% | ±5% | ±5% | 0 |
| Bias Disp. Error | +5% | +5% | +5% | 0 |
| Random Error Seed | 13 | 13 | 13 | - |
| Mode | Generalized Masses ($Lb/Sec^2/In.$) | | | |
| 1 | 8.474 | 8.464 | 8.518 | 8.534 |
| 2 | 4.556 | 4.510 | 4.492 | 4.449 |
| 3 | .488 | .487 | .487 | .495 |
| 4 | 1.150 | 1.151 | 1.103 | 1.087 |
| 5 | .596 | .597 | .595 | .630 |
| 6 | .722 | .724 | .777 | .744 |
| 7 | 1.182 | 1.113 | 1.159 | 1.177 |
| 8 | 1.232 | 1.242 | 1.215 | 1.412 |
| 9 | .797 | .743 | .789 | .786 |
| 10 | 1.203 | 1.043 | -.564 | .043 |
| 11 | .093 | .104 | .0103 | .172 |
| 12 | 1.177 | 1.119 | 1.147 | 1.050 |

** From 20 x 20 Specimen

## Response From Identified Model

One of the most essential requisites of relating a discrete parameter system to a continuous system is model response fidelity over a given frequency range of interest. The finite degree of freedom model must accurately reproduce the dynamic response of the infinite degree of freedom structure over a specific number of modes. Figures 2a and 2b show typical real and imaginary driving point acceleration response respectively for the five point model. The "exact" curve represents the simulated experimental data for the twenty point structure, obtained with zero error. The frequency range encompasses the first five elastic natural frequencies. Figures 3 and 4 present similar results for typical nine and twelve point models, respectively. The computer experiments for which results are presented incorporated a ±5 percent random and a +5 percent bias on the real and imaginary displacement mobility data. As evidenced by the figures, the various models yielded satisfactory reidentification of the twenty point specimen simulated dynamic response data.

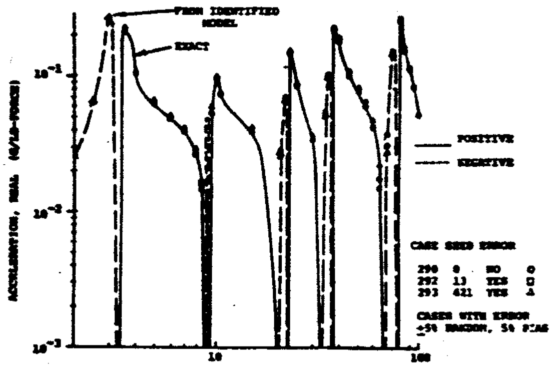


Figure 2a. Effect of Error on Five-Point Model Identification of Real Acceleration Response; Driving Point at Hub

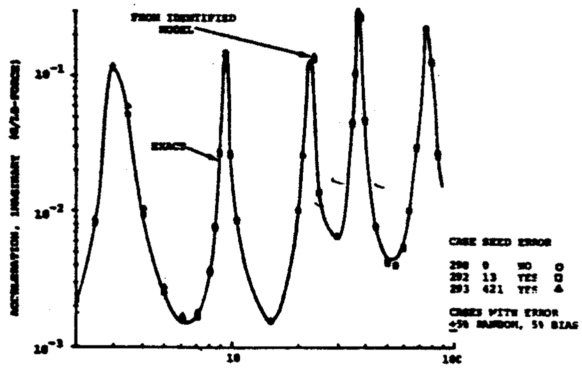


Figure 2b. Effect of Error on Five-Point Model Identification of Imaginary Acceleration Response; Driving Point at Hub

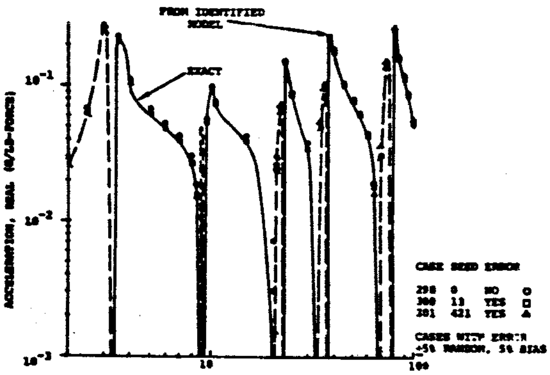


Figure 3a. Effect of Error on Nine-Point Model Identification of Real Acceleration Response; Driving Point at Hub

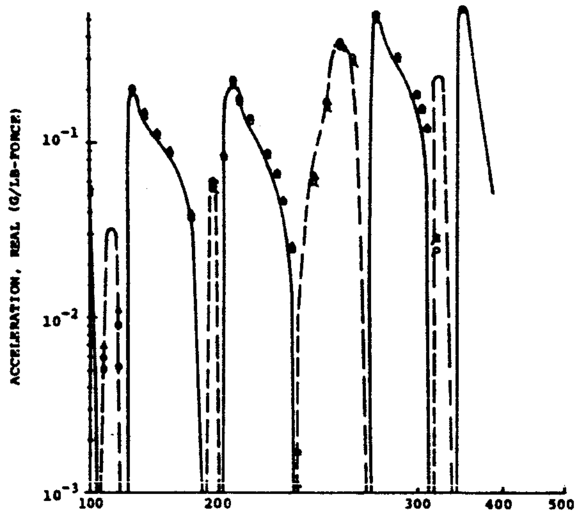


Figure 3a - Continued

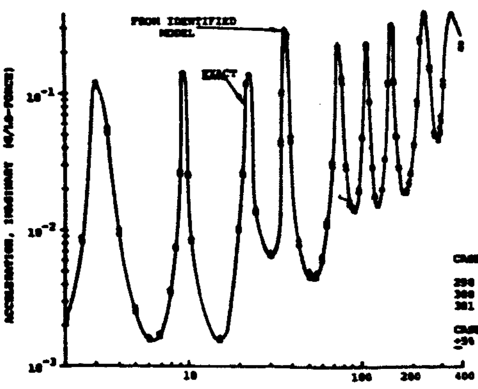


Figure 3b. Effect of Error on Nine-Point Model Identification of Imaginary Acceleration Response; Driving Point at Hub

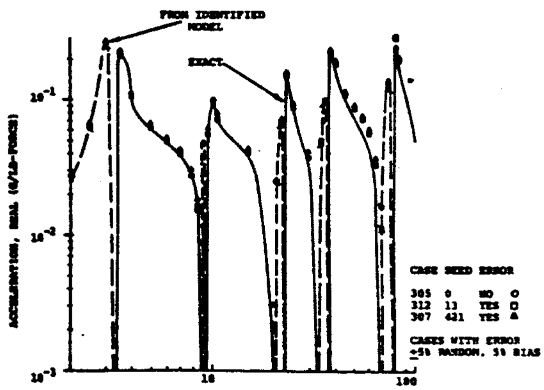


Figure 4a. Effect of Error on Twelve-Point Model Identification of Real Acceleration Response; Driving Point at Hub

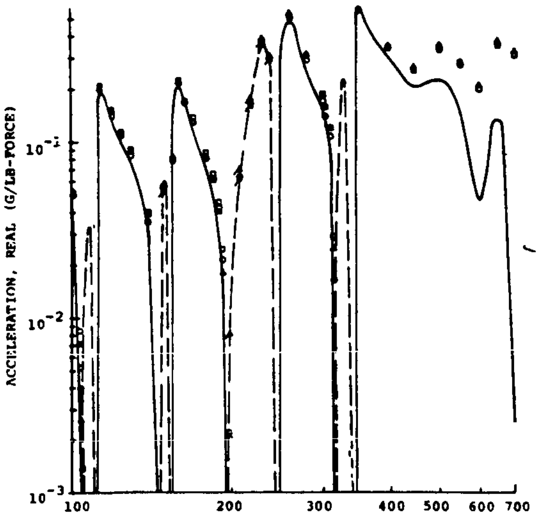


Figure 4a - Continued

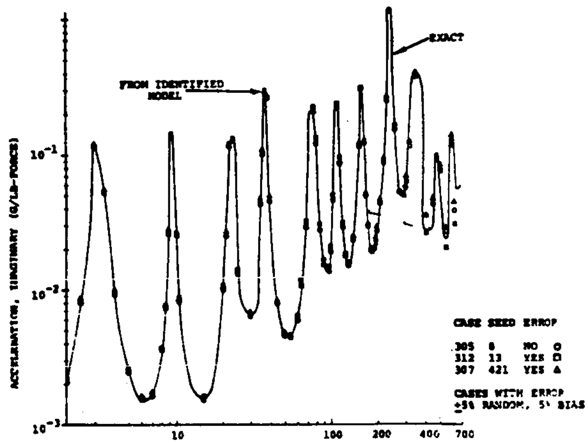


Figure 4b. Effect of Error on Twelve-Point Model Identification of Imaginary Acceleration Response; Driving Point at Hub

## Conclusions

1. Single point excitation of a structure yields the necessary mobility data to satisfactorily determine the mass, stiffness and damping characteristics for a mathematical model having less degrees of freedom than the linear elastic structure it represents.

2. The method does not require an intuitive mathematical model and uses only a minimum amount of impedance type test data.

3. The eigenvector or mode shape associated with each natural frequency is also determined.

4. Computer experiments using simulated test data indicate the method is insensitive to the level of measurement error inherent in the state-of-the-measurement art.

## References

1. USAAMRDL Technical Report 70-6A, THEORY OF STRUCTURAL DYNAMIC TESTING USING IMPEDANCE TECHNIQUES, Flannelly, W.G., Berman, A. and Barnsby, R. M., U. S. Army Air Mobility Research and Development Laboratory, Fort Eustis, Virginia, June 1970.

2. USAAMRDL Technical Report 72-63A, RESEARCH ON STRUCTURAL DYNAMIC TESTING BY IMPEDANCE METHODS - PHASE I REPORT, Flannelly, W.G., Berman, A. and Giansante, N., U. S. Army Air Mobility Research and Development Laboratory, Fort Eustis, Virginia, November 1972.

3. Stahle, C.V., Jr., PHASE SEPARATION TECHNIQUE FOR GROUND VIBRATION TESTING, Aerospace Engineering, July 1962.